



Investigation and FEM analysis of mineshaft rope safety platforms in underground mining

by C. Dębek*, A. Wasilewicz†, and T. Czyż‡

Synopsis

Both Polish and European hard coal mining nowadays faces the need of deepening shafts (significantly in some cases) or extending mining hoists, due to the exploitation of deeper coal deposits.

In order to protect the crew working within a shaft, rope safety platforms (artificial shaft bottoms) are employed. Old solutions, based on rigid steel constructions with the external damping layers made of e.g. slag and up to several tens of metres long, are intended to absorb the energy of approximately 5 t mass falling a distance of 700 m. However, current requirements often assume a drop of 20 t to a depth of 1000 m or even more.

More modern safety platform structures, made of one or more support rings with steel ropes stretched on them (rope platforms), are more compact (up to 3 m high) and lighter than traditional solutions. Multi-ring rope platforms with additional damping layers filling the empty spaces between the ropes are able to absorb sufficient energy to meet the current requirements.

Single- and double-ring platforms have been employed in Poland to absorb the energy of approximately 5 t dropping to a depth of 900 m. They have been developed (and some have already been implemented) by SADEX Ltd. and are protected by various patents and patent applications.

This paper presents a design for a triple-ring platform structure with six rope nets. FEM analysis was used to model the performance of the platform. According to the simulation, a 20 t mass falling from 1000 m (>100 m/s) will destroy all the nets, breaking most of the ropes and deforming the support steel boards placed on the nets, but will ultimately be stopped by the platform, as its kinetic energy falls to zero.

Keywords

rope safety platform, artificial bottom, underground mining, shaft, mining hoist.

Introduction

Both Polish and European hard coal mining are nowadays facing the need to significantly deepen the operating shafts or extend operating mining hoists, due to the exploitation of deeper coal deposits. In deepening shafts and extending operating mining hoists it is necessary to use safety platforms (protection platforms, protective platforms, main platforms, artificial shaft bottoms, shaft corks). An artificial bottom is supposed to wholly or partially separate the shaft section with the operating mining hoists from the section being deepened, where the shaft deepening teams or the teams assembling the equipment of an extended

hoist section are employed (Kostrz, 1972; Journal of Laws, 2002; Carbogno and Żołnierz, 2011).

Due to the increased depths where such platforms are used and the possibility that four or five times heavier objects may fall into the shaft compared to the past, safety platforms meeting these new requirements are needed (Carbogno and Żołnierz, 2011).

The Ordinance of the Minister of Economy of 28 June 2002 on occupational health and safety, traffic operation, and specialist fire protection measures in underground mines, which became binding for the Polish mining industry on 2 September 2002, in appendix no. 4 entitled 'Detailed principles for traffic in the excavations', Chapter 5 – paragraph 5.15.11 – 'Artificial shaft bottom' – presents the following requirements for designing and construction of a shaft artificial bottom: *Point 5.15.11.2.2. If the shaft section located beneath the artificial bottom operates another hoist or people are to be employed in such section, it is required to mount one safety platform or other safety devices there as well as one inspection platform approximately 3 m beneath it. The safety platform or another protective device shall have the structure calculated to bear the load of a loaded mine truck falling from the shaft top. The calculations shall prove that the platform will not be permanently deformed. The platform shall be covered with a damping layer. In the case of shafts with a skip hoist the assumed falling weight shall be 1/10 of the skip utility weight, assuming that the weight cross-section is 0.5 m² (Journal of Laws, 2002).*

* Institute for Engineering of Polymer Materials and Dies, Piastów, Poland.

† SADEX Sp. Ltd, Rybnik, Poland.

‡ MESco, Tarnowskie Góry, Poland.

© The Southern African Institute of Mining and Metallurgy, 2017. ISSN 2225-6253. Paper received Feb. 2014; revised paper received Dec. 2016.

Investigation and FEM analysis of mineshaft rope safety platforms

The solutions modelled on German structures described in the TASS requirements are most popular in Poland. These are steel structures with an external damping layer made of *e.g.* granulated slag with an inspection platform placed approximately 3 m below it. Such a platform is made of two basic elements: a rigid structural basis and the damping layer. The rigid platform part is made of steel double-T-bar carriers (at least one layer) covering the shaft cross-section. It usually uses I 300 to I 500 T-bars. The platform made of the carriers supports transverse support joists (two joists minimum) fixed in the shaft lining and based on some extra stays bearing the vertical load to the shaft lining. Two types of carrier platform are used, depending on the impact load. In the first option the carriers are mounted in the shaft lining while in the other, the carriers are placed on joists. In the latter the total load is borne by the joists and stays Kostrz, 1972; Walewski, 1965).

For example, a platform made for the following parameters: falling weight of 3 t (1/10 of skip load), fall height of 700 m, shaft diameter of 6 m, is made of sixteen I 340 carrier beams, carrier base of 360 mm, two joists made of I 500 carriers, and four I 340 stays. The platform's total weight is 93.8 t, the steel elements weight 20 t, the damping layer made of a 7 m thickness of boiler slag has a mass of 73.8 t, and the total height without the inspection platform is 12 m.

The increasingly intense excavations by individual mining enterprises as well as the increased weight of extracting machines necessitated an adjustment of the technical capabilities of the vertical transport. Therefore the mining hoists used to date have been constructed or modernized in order to transport machines or sets of excavation machines of up to 20 t mass. If the works related to deepening an operating shaft or extending a mining hoist concern a shaft with the parameters described above and the area for the safety platform commissioned for the development prior to the works commencement (meeting the provisional requirement) usually reaches ≤ 3 m, the compactness of the structure is crucial. Platforms calculated to bear such high loads have not been used yet in Poland.

For comparison, assuming the more commonly required requirements: a falling mass of approximately 18 t, fall height of ≥ 700 m, shaft diameter of 8 m, and height of the damping layer of 9 m, I 1000 bars shall be used as basic carriers, much larger than previously. The total platform height will then exceed 16 m and with the inspection platform it will reach approximately 20 m. The size of the complete platform makes it difficult to place it in the deepened shaft. Basic carrier bars may be reduced to I 500 to I 600 provided that the damping layer is 18 m thick, resulting in the platform structure length of approximately 25 m (Carbogno and Żołnierz, 2011).

The most popular safety platforms in Poland weigh ≥ 100 t themselves in case of a fall height > 700 m and the structure height exceeds 20 m, therefore the compactness criterion excludes these solutions. The obvious disadvantage of such solutions, besides their height, is the weight of the platform and the damping layer. Moreover, the slag used slakes, transforming into a compact mass and losing its damping quality. The platform is also difficult to remove following the completion of shaft deepening or extension (Hansel *et al.*, 1989a, 1989b).

Due to their size, cost, and assembling capabilities, such solutions are appropriate for former requirements, where the weight of the falling objects was approximately 5 t and the fall height was 700 m. In case of the requirements set currently by the mines, with the mass reaching up to 20 t and the fall height ≥ 1000 m, such solutions are insufficient.

Safety platforms using the concept of steel rope nets are also employed in Poland. The first platforms of that type were developed in 1982 at the Institute of Iron Ore Mining in Krivvi Rih in Ukraine. The Ukrainian mining industry is the one most experienced with the use of rope platforms, and various constructions have been developed depending on the requirements. The development of safety platforms with a compact structure based on rope nets was suspended in Ukraine when they reached the following parameters: fall height of 600 to 1000 m and the fall mass not exceeding 5 t (Carbogno and Żołnierz, 2011).

Several safety platforms with two-level rope nets have been used in Poland in recent years. The basic advantage of such platforms is their significantly smaller size compared to the former rigid structures. Such solutions are compact, light, and easy to assemble and disassemble. They are useful if the falling mass does not exceed 4 t and the fall height does not exceed 1000 m. In case of heavier masses from 10–20 t, the fall energy necessitates the application of more and larger diameter ropes and relatively heavier loadbearing rings of the platform. To absorb the fall energy it is necessary to use a platform with three or more rows of double nets, making the platform heavier and higher. If the works related to deepening an operating shaft or extending an operating mining hoist concern the strictest requirements, and since the area for the platform development is usually smaller than 3 m, the compactness of the structure is crucial (Carbogno and Żołnierz, 2010; Gorgol and Jeglorz, 2010; Hansel 1985).

The safety platform mass and dimensions depend on the mass of the falling object and the fall height. For example, the weight of a complete half-platform with two-level net designed for a fall height of 720 m and fall mass of 3.4 t, with a shaft diameter of 9 m is approximately 40 t and its height reaches 1 m. One of the technical requirements, namely the structure compactness, meets the solution entitled 'Platform for protecting the bottom of an underground mine shaft' (Sala *et al.*, 2006a), however, the solution does not absorb the fall energy of heavy masses for depths exceeding 1000 m, which is essential under the provision quoted above (Journal of Laws, 2002).

The rope platforms in Poland are manufactured by SADEX Ltd, based on the projects developed by the Measurements Mining Company Ltd and the AWAN partnership, cooperating with the Institute of Mining Mechanisation of the Silesian University of Technology in Gliwice (Carbogno and Żołnierz, 2010; Gorgol and Jeglorz, 2010). The SADEX company is the leader in rope platform solutions in Poland. It has implemented safety rope platforms protected by patents and patent applications for the following parameters: falling mass of 3 t and fall height of 700 m (Sala *et al.*, 2006a, 2006b; Sala and Wasilewicz, 2012; Ryszka and Wasilewicz, 2012).

To sum up, the safety platforms used to date were designed for a falling mass not exceeding 4 t with the fall height not exceeding 900 m. The use of mining hoists with

Investigation and FEM analysis of mineshaft rope safety platforms

large cages capable of transporting 15 or 17 t and heavier masses, potential fall heights exceeding 1000 m, as well as stricter requirements concerning the dimensions of the platform itself set new requirements concerning the design and construction principles of safety platforms.

A useful solution is the rope-based systems that are already in use. To meet the current maximum requirements, multi-ring structures of platforms with several levels of rope nets combined with energy absorbers, *e.g.* elastomer layers filling the empty spaces in the nets, are being considered (Dębek and Wasilewicz, 2013, 2014). Currently the work is being financed by funding under grant no. PBS1/B2/1/2012 in the Program for Applied Research by SADEX Ltd in cooperation with the Institute for Engineering of Polymer Materials and Dyes, Elastomer and Rubber Technology Division, leading the project.

This paper presents the structure and analysis according to the FEM methodology concerning a triple-level rope safety platform hit by a 20 t mass falling at a velocity of ≥ 100 m/s, reflecting the shaft fall height of 1000 m. Future publications will present results obtained for platforms equipped with elastomer damping layers.

Structure of the safety platform

The diagram of the safety platform (artificial shaft bottom) under analysis is shown in Figure 1.

The safety platform has been designed according to the following requirements:

- Mass of the falling object: 20 t
- Depth of the artificial bottom: 1050 m
- Shaft diameter: 8.5 m

The safety platform is made of three steel rings, each composed of eight segments. One of the segments – no. 1 – is equipped with the so-called 510 mm wide locking cover allowing closing of the ring inside the shaft. Additionally, a 10 mm thick assembly gap to adjust any inaccuracies in the correct development has been provided.

The horizontal segment sheets are of various thicknesses depending on the location of the segment within the ring. Segments 2 and 2, the corner ones with ropes mounted in two directions, are the thickest. This is due to the highest complex tensions being present at that segment of the ring.

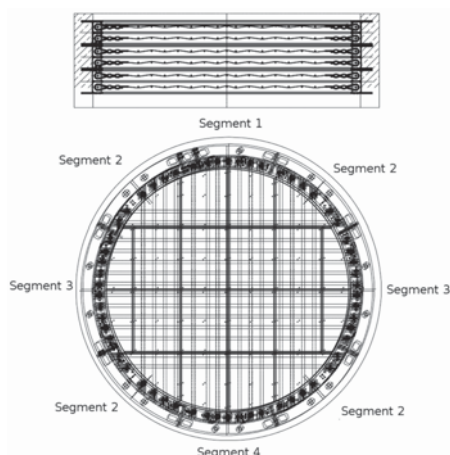


Figure 1—Diagram of the safety platform

The segments of a ring are assembled with 4/7 pressed M36 bolts (class 10.9) and nuts (class 10) (vertical threaded fittings). The vertical threaded fittings are located on the ring circumference at the spots of the lowest complex tensions. Assembly holes have been provided in the top plate and in the vertical coating to allow the threaded fitting. The holes in the top plates, on the other hand, are intended for concrete filling of the spaces behind the ring. In such a case the holes in the vertical coating shall be then covered with a 13×120×250 mm plate (on the shaft lining side).

Individual rings are assembled with class 8.8 M36 bolts and class 8 nuts. To facilitate the assembly, the bolt holes are oval and have dimensions of 38×43 mm.

Two 32 mm diameter steel rope nets are assembled to each ring. In each net the ropes are intertwined perpendicularly, creating a rope net. The rope ends pass through steel discs, are tightened with welded 'SADEX' jaws, and assembled to the steel ring with 60 mm diameter pins. Each pin is secured with an M12 bolt, recommended to be wrenched on a tightening thread glue, *e.g.* Loctite.

The top net of the top ring is covered with two crossing layers of used conveyor belt. Additionally, to obtain an efficient load distribution to more net holes, 10 mm steel plates reinforced with a lattice of T-bars with dimensions of 100×100×11 mm are placed on the nets. The plates are assembled to the rubber belts with 12 mm diameter wood screws.

Basic parameters of the artificial bottom:

- Rope type: Ø 32 WS 6×36+Ao-Z/s-n-II-g-1770
- Number of ropes in one basic net: 58
- Rope length in one basic net without surplus length for rope holes: 434 m
- Rope length in one basic net with surplus length for rope holes: approx: 550 m
- Number of rings: 3
- Number of segments within one ring: 8
- Mass of the heaviest element (segment 3): 4.615 t
- Dimensions of the largest element (segment 3): 780 × 1111 × 4205 mm
- Height of a single ring: 780 mm
- Height of the artificial shaft bottom: 2340 mm
- Mass of the whole artificial shaft bottom: approx. 12.1608 t.

Geometric model of the safety platform

The ring is composed of four types of segments. Figure 2 shows a 3D model of segment 1. The solid model of ring segments has been replaced with the shell model, with the element thickness provided as a parameter.

The shell mode of a board supported with T-bars is shown in Figure 3. Such boards are placed on each rope net.



Figure 2—3D model of segment 1 of a safety platform ring

Investigation and FEM analysis of mineshaft rope safety platforms

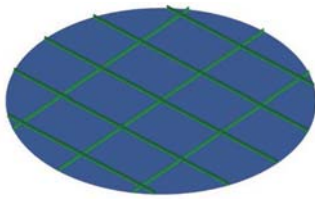


Figure 3—Shell mode of a 100 x 100 mm T-bar board

Figure 4 presents a 3D model of a simplified mechanized roof segment hitting the deck.

The rope net has been developed directly from ready-made products and there is no geometric model thereof.

FEM Model

The shell geometry has been divided into ready-made elements. Table I shows the types of elements used for analysis, number of nodes, and elements of each part of each type. The whole model comprises three segments no. 1, three segments no. 3, three segments no. 4, 12 segments no. 2, six T-bar boards, six rope nets, one cover segment, pins, and bolts.

Figures 5 and 6 show the discretization of selected model elements.

The whole numeric model is shown in Figure 7. The model comprises 391 082 shell elements and 39 504 beam elements. There are 471 319 nodes in the model.

Connections

The rope nets are connected to the ring with pins, as modelled with the Ø 60 mm beam elements (Figure 8). The pin beams are connected to the ring boards with Constrained_Nodal_Rigid_Body elements, providing a perfectly rigid connection.

The ring segment connections have been provided with Ø 36 mm beam elements.

Contacts

The interactions between the elements that have been defined in the model are provided in Table II.

Properties of materials and adopted material models

Ropes

The virtual rope modelled was Ø 32 WS 6x36+Ao-Z/s-n-II-g-1770. A Warrington-Seale rope with the diameter of 32 mm,



Figure 4—Simplified 3D model of the object impacting the platform – mechanized cover segment



Figure 5—Discretization of ring segment 2

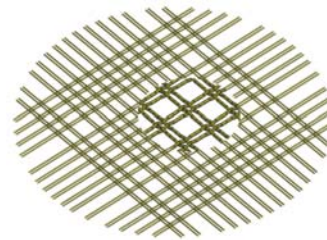


Figure 6—Discretization of the rope net

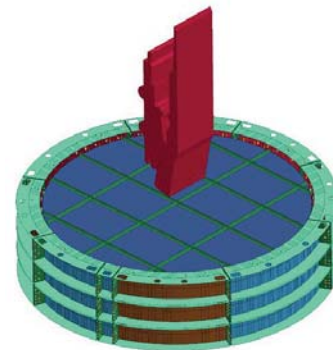


Figure 7—Complete numerical model of the rope platform

| Table I | | | | |
|-------------------------|---------------|----------------------|--------------------|-----------------|
| Model discretization | | | | |
| Part name | Item type | Kind of item LS-DYNA | Number of elements | Number of nodes |
| Segment 1 | Shell 4 nodes | Type 16 | 11792 | 14455 |
| Segment 2 | Shell 4 nodes | Type 16 | 12442 | 14568 |
| Segment 3 | Shell 4 nodes | Type 16 | 15684 | 20721 |
| Segment 4 | Shell 4 nodes | Type 16 | 10131 | 12642 |
| T-bar boards | Shell 4 nodes | Type 2 | 11438 | 12419 |
| Mechanized roof segment | Shell 4 nodes | Type 2 | 13277 | 13259 |
| Rope nets | Beam 2 nodes | Type 1 | 6244 | -- |
| Pins | Beam 2 nodes | Type 9 | -- | -- |
| Bolts | Beam 2 nodes | Type 9 | -- | -- |

Investigation and FEM analysis of mineshaft rope safety platforms

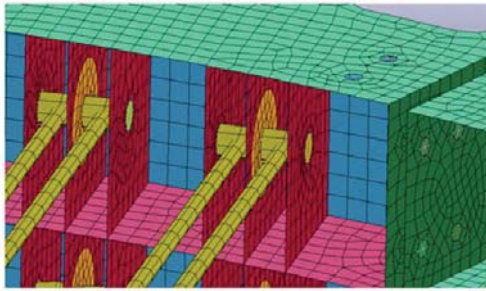


Figure 8—Connection of the rope net to the ring

As fiber core, six strands 36 wires each, lang's lay rope was used. The maximum strength according to the test is 689 kN. The mass of 1 m of the rope is 4.2 kg.

The model material parameters were established based on the load deformation characteristics obtained in a statistical rope-breaking test using a 3040 mm long testing segment tensile test.

The tensile test characteristics were replaced with the tension – deformation characteristics assuming the rope cross-section area $A = 804.248 \text{ mm}^2$.

The tension characteristics by plastic deformation were determined. This deformation is to be directly specified as material data.

The plastic deformation upon rupture was calculated based on the deformation breaking the first three strands and increased by 20% based on the work of the unbroken strands. $E_p = 0.0189$.

The area under the curve of the virtual characteristics following the rupture of the three strands covers approximately 20% of the area under the curve until the three first strands rupture. The other rope material parameters are as follows:

E – Young's modulus: 28.58771 GPa

ν – Poisson's ratio: 0.3 (negligible since the analysis concerns bar-based elements).

Following multiple numerical tests the following material model has been adopted: Mat24_Piecewise_Linear_Plasticity.

Steel boards, T-bars, loadbearing ring segments

The following model dependent on the deformation velocity was adopted for ring boards and segments: Mat15_Johnson_Cook. The model parameters were determined for the S355J2 steel, based on tests performed at the Institute of Road Transport.

Steel samples were tested within deformation velocity range of up to 2500 s^{-1} using the modified split Hopkinson pressure bar method, shown schematically in Figure 9. The cylindrical sample was placed between two 1 m long bars with a diameter of 20 mm made of steel of high machinability (maraging steel). The bar projectile (5) was propelled in a pneumatic launcher (1) and impacted the initiating bar (8) with the V0 velocity generating elastic wave propagating along the bar. When the wave reached the bar front, it caused movement that deformed the sample. Part of the wave was reflected and propagated in the opposite direction along the initiating bar, while the remaining part of the wave passed through the sample to the transmission bar (9) and moved along the bar until it reached the damper assembled on its end, which absorbed the wave. The initial projectile velocity was measured by the short time meter recording the time in which the projectile passed 80 mm. The time measurement was started with an optoelectronic system consisting of two diode and photodiode couples. The mechanical waveform was recorded with a strain wire bridge circuit. To average the mechanical waveform and eliminate the effects of bar buckling, the deformation was measured with two strain gauges glued symmetrically on the bar circumference. Based on the passing $\varepsilon T(t)$ and reflected $\varepsilon R(t)$ waveforms recorded with a digital oscilloscope, and knowing the cross-section areas of bars A and of the sample A_S , as well the velocity of the elastic wave propagating in the bars C_0 and the sample length L , it was possible to determine the timelines of the tension $\sigma(t)$, deformation $\varepsilon(t)$, and deformation velocity $\dot{\varepsilon}(t)$ in the sample based on the following correlation:

$$\sigma(t) = E \left(\frac{A}{A_S} \right) \varepsilon_T(t) \quad [1]$$

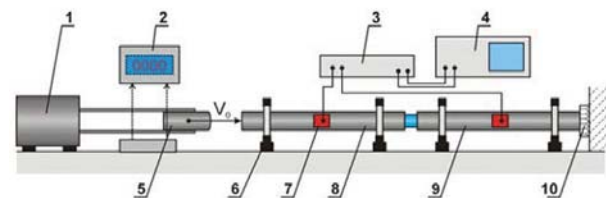


Figure 9—Apparatus for the modified split Hopkinson pressure bar method; 1 – pneumatic launcher, 2 – optoelectronic projectile velocity measurement system, 3 – wideband strain wire bridge, 4 – digital oscilloscope, 5 – projectile, 6 – bar bearing, 7 – strain gauges, 8 – initiating bar, 9 – transmission bar, 10 – vibration damper

Table II

Interaction within the model

| Contact parts | Type of contact LS-DYNA | Friction coefficient |
|-------------------------------------|------------------------------|----------------------|
| Ropes with themselves | Automatic_General | 0.1 |
| Ropes with mechanized roof segment | Automatic_Nodes_to_Surface | 0.1 |
| Ropes with T-bar boards | Automatic_Nodes_to_Surface | 0.1 |
| Boards with themselves | Automatic_Single_Surface | 0.1 |
| Flange of segments | Automatic_Single_Surface | 0.1 |
| Outer shelf of segments | Automatic_Single_Surface | 0.1 |
| Mechanized roof segment with boards | Automatic_Surface_to_Surface | 0.1 |
| T-bars with desks | Tied_Surface_to_Surface | – |

Investigation and FEM analysis of mineshaft rope safety platforms

$$\varepsilon(t) = -\frac{2C_0}{L} \int \varepsilon_R(t) dt \quad [2]$$

$$\dot{\varepsilon}(t) = \frac{d\varepsilon(t)}{dt} = -\frac{2C_0}{L} \varepsilon_R(t) \quad [3]$$

The Johnson-Cook equation is as follows:

$$\sigma(\varepsilon, \dot{\varepsilon}, T) = \left(A + B\varepsilon^n \right) \left(1 + C \ln \left(\frac{\dot{\varepsilon}}{\dot{\varepsilon}_0} \right) \right) \left(1 - \left(\frac{T - T_R}{T_m - T_R} \right)^m \right) \quad [4]$$

with the tension correlated with the plastic deformation, deformation velocity, and temperature.

The ratios for the simulation model are presented in Table III.

Additionally, the following parameters of the material destruction equation have been added to the Mat15 model:

$$\varepsilon^f = \max \left([D_1 + D_2 \exp D_3 \sigma^*] [1 + D_4 \ln \dot{\varepsilon}^*] [1 + D_5 T^*], \text{EFMIN} \right) \quad [5]$$

with ε^f for the breaking deformation. The D_1 to D_5 parameters have been adopted based on the method (Johnson and Cook, 1985) developed for 4340 steel and are shown in Table IV.

Destruction and deletion of the ready-made element occurs when the D parameter:

$$D = \sum \frac{(\Delta \varepsilon^p)}{\varepsilon^f} \quad [6]$$

is unity.

The roof segment material is assumed to be perfectly rigid.

Pins and bolts

The material adopted for the pins and bolts relates to the beam elements representing pins and bolts. This is the Mat100_Spotweld material with the parameters shown in Table V.

Initial and boundary conditions and settings of the analysis

- *Initial conditions*—The only initial condition was the roof segment velocity of 100 m/s.
- *Boundary conditions*—The bottom surface of the last ring was fixed in the Z direction.
- *Setting of the analysis*—Analysis period of 150 ms. Damping for the rope net Damping_Frequency_Range set

| A | B | n | C | m | $\dot{\varepsilon}_0$ | T_0 | T_m |
|-----|-----|------|------|-----|-----------------------|-------|-------|
| 667 | 233 | 0.58 | 0.02 | 0.6 | 0 | 296 | 1800 |

at 12% of the critical damping within the frequency range 2e-5-2e-4 Hz according to Stolle *et al.* (2010).

FEM analysis results

Figures 10–12 show visualizations of the impact analysis results for a mechanized roof segment with a mass of 20 t falling with a velocity of 100 m/s. The roof segment impacts the platform eccentrically with its smallest area – the worst possible impact conditions. Figures 10 and 11 show half cross-sections at the commencement of analysis and when the kinetic energy of the roof segment falls to zero (within 120 ms).

| D1 | D2 | D3 | D4 | D5 |
|------|-----------|-------|-------|------|
| 0.05 | 1.03.1944 | -2.12 | 0.002 | 0.61 |

| Young's modulus | Density | Poisson's ratio |
|-----------------|----------------------------|-----------------|
| 210 GPa | 7.85e-6 kg/mm ² | 0.3 |

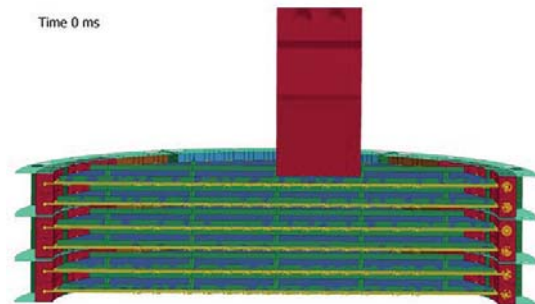


Figure 10—The platform view in cross-section at 0 ms

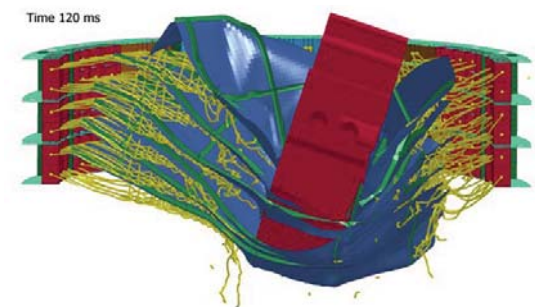


Figure 11—Platform cross-section at the point when the impacting cover stopped (120 ms)

Investigation and FEM analysis of mineshaft rope safety platforms

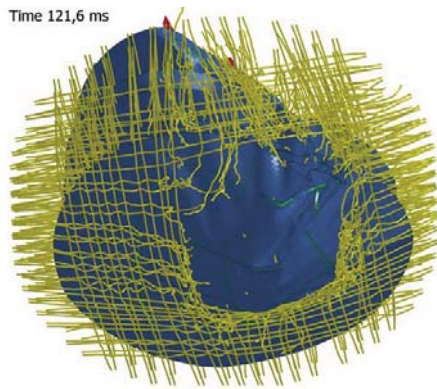


Figure 12—Bottom view of the platform boards and ropes only

Figure 12 show the platform bottom view at the roof segment stopping point. The figure shows only the steel boards and ropes. The impacting roof segment halts when stuck in the steel plates supported by T-bars and its kinetic energy falls to zero. The steel boards supported by T-bars are deformed and a large number of ropes in particular segments are ruptured.

Figure 13 shows the amount of energy absorbed by individual model segments based on their internal energy increase. Unexpectedly, according to the FEM analysis, most of the energy is absorbed by the steel board (B) deformation, then T-bar (C) deformation, and finally steel rope rupture (A). The ring segments (D-Q) are less important.

Due to the technical and economic issues related to the platform construction, the calculations were carried out for the rings with reduced thickness of the ring segment steel plates. The following dimensions were amended in the model with the new ring plate thickness:

- Thickness of the flanges of segments 1, 3, and 4 reduced from 50 mm to 30 mm
- Thickness of the flanges of segment 2 reduced from 60 mm to 40 mm.

Figure 14 shows maximum tensions in the ring with the initial thickness of the steel plates. Figure 15 shows the maximum tensions in the ring with the reduced steel plate thickness. Compared to the steel boards, ropes, or T-bars, the rings absorb little energy, as a result of the rope destruction conditions, since the ropes bear no greater ring loads than those that the ropes themselves can bear. The rings deform resiliently within almost their total volume. The minor reduction in the tension strength above the plasticity limit of 667 MPa is not dangerous and the rings may be used again with a new rope net. The case when the ring is anchored in the shaft wall has not been tested; in the test model the ring is placed on a no-friction support.

The results obtained for the rings with the reduced steel plate thickness indicate that the thickness reduction is allowable and will not result in any significant changes in the system behaviour.

Conclusions

This report presents a simulated impact of a mechanized roof

segment falling with velocity of 100 m/s onto a rope safety platform. Within the simulation time of 150 ms the roof segment destroys all the rope nets and deforms the boards supported with T-bars. The roof segment is halted when stuck in the boards and nets and after its kinetic energy falls to zero. The deformation of the boards supported with the T-bars absorbs the largest amount of energy, and the ropes the second-largest amount. Compared to the boards, the ring absorbs minor amounts of energy. This results from the rope destruction condition, since the ropes are not capable of bearing more ring load than the load they are capable of

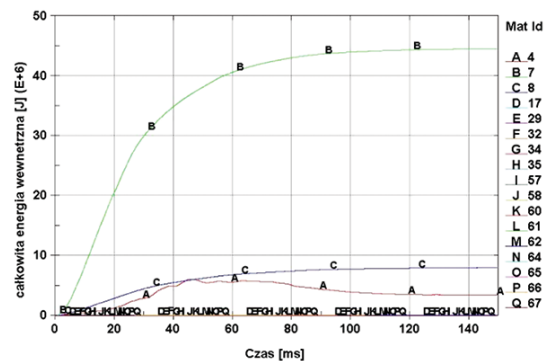


Figure 13—Internal energy of individual model segments, A – ropes, B – boards, C – T-bars, D-Q – ring segments

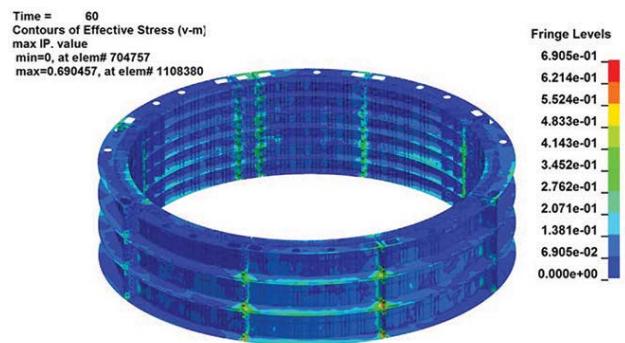


Figure 14—View of the maximum tensions applied to the ring with the initial steel sheet thickness, unit (GPa)

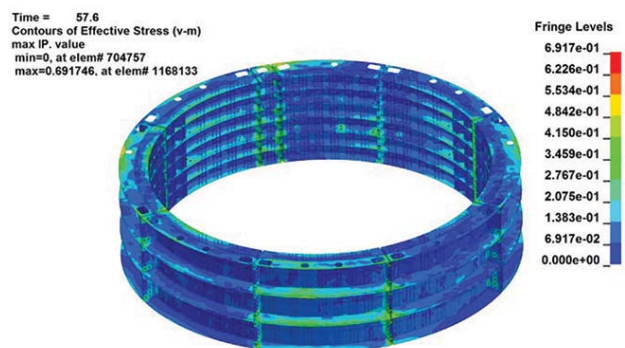


Figure 15—View of the maximum tensions applied to the ring with the reduced steel sheet thickness, unit (GPa)

Investigation and FEM analysis of mineshaft rope safety platforms

bearing themselves. The rings deform resiliently within their almost entire volume. The minor reduced tension strength above the plasticity limit of 667 MPa is not dangerous and the rings may be used again with a new rope net.

Analysis of the results for the ring with reduced steel plate thickness indicates that the plate thickness reduction is allowable and will not result in a significant change in ring behaviour change.

The scale of the model under analysis, as well as the velocity of forces, affects the limitations related to the experimental material tests for the safety platform components.

They also provide a basis of model uncertainty including:

- The material model of the rope based on statistical tests
- The rope damping model assumed based on the tests for smaller ropes
- A Johnson-Cook model of destruction for boards, T-bars and ring assumed for the 4340 steel
- Friction ratio of model components assumed as 0.1 for the whole model.

The above uncertainties do not exclude the compliance of the results with reality. The assumptions made ensure that the results are on the conservative side.

The simulation presented here constitutes the first stage of testing for the development of a rope safety platform meeting current requirements – absorbing the energy of an impact by a 20 t object falling from a height of 1000 m.

The construction under analysis fails to meet the requirement set forth in the Journal of Laws (2002) for the assumed impact energy. Stronger ropes, and possibly additional damping layers filling free spaces in order not to increase the platform's total height, are required.

Acknowledgement

This work was funded by the Program for Applied Research (no. 177848 application, agreement PBS1/B2/1/2012).

References

- CARBOGNO, A. and ŻOŁNIERZ, M. 2010. Technical documentation of safety platform for the first shaft in JSW KWK Budryk and the calculation of the rope safety platform. Unpublished documents, PMG Sp. z o.o and Sadex Sp. z o.o.
- CARBOGNO, A. and ŻOŁNIERZ, M. Zagadnienie projektowania pomostów bezpieczeństwa stosowanych podczas pogłębiania szybów (The problem of designing safety platforms used during the deepening of the mine shafts). *Proceedings of 6 Międzynarodowa Konferencja Naukowo-Techniczna, Transport Szybowy*, Ryto, Poland, 19–21 September 2011.
- DEBEK, C. and WASILEWICZ, A. 2013. Damping material intended for the damping layer in the safety rope platforms. Patent Appl. PL no. P. 405751.
- DEBEK, C. and WASILEWICZ, A. 2014. Elastomeric material intended for the damping layer in safety rope platforms. Patent Appl. PL no. P. 408411.
- GORGOL, L. and JĘGLORZ, D. 2010. The technical documentation and construction of safety platform of the first shaft in JSW KWK Budryk. Unpublished documents, PMG Sp. z o.o and Sadex Sp. z o.o.
- HANSEL, J. 1985. Zadania dydaktyczne, naukowo-badawcze oraz twórczość wynalazcza Katedry Transportu Linowego (Didactic, research tasks and inventive work of Department of Transport Rope), *Zeszyty Naukowo-Techniczne KTL* Nr 4, Kraków.
- HANSEL, J., WÓJCIK, M., CICHOCIŃSKI, A., HORA, M., JARNO, L., MENCEL, Z., ŚMIAŁEK, Z., WRÓBLEWSKI, Z., ZYMAN, Z., and KONIECZNY, S. 1989a. Artificial bottom for shaft ways. PL Pat. 146952.
- HANSEL, J., WÓJCIK, M., ŚMIAŁEK, Z., HORA, M., BERBEĆ, S., KONIECZNY, S. and MENCEL, Z. 1989b. Artificial pit bottom. PL Pat. 148130.
- JOHNSON, G.R. and COOK, W.H. 1985. Fracture characteristics of three metals subjected to various strains, strain rates, temperatures and pressures, *Engineering Fracture Mechanics*, vol. 21, no. 1. pp. 3-148.
- JOURNAL OF LAWS. 2002. No. 139, item 1169, appendix no. 4. Detailed principles for traffic in the excavations, chapter 5, point 5.15.11. Artificial shaft bottom, pp. 101–102.
- KOSTRZ, J. 1972. Pogłębianie szybów i roboty szybowe. *Górnictwo t. VI* cz. 3 (The deepening of shafts and shaft works). *Mining*, vol. VI, part 3. Wydawnictwo Śląsk, Katowice.
- RYSZKA, B. and WASILEWICZ, A. 2012. Shaft mining safety platform. PL Pat. 397827.
- SALA, M. and WASILEWICZ, A. 2012. Shaft mining safety platform. PL Pat. 397826.
- SALA, M., CARBOGNO, A., and CZARNECKI, A. 2006a. Platform for protecting the bottom of an underground mine shaft. PL Pat. 191899.
- SALA, M., CARBOGNO, A. and CZARNECKI, A. 2006b. Half-platform for protecting an underground mine shaft bottom. PL Pat. 192107.
- STOLLE, C.S. and REID, J.D. Modeling wire rope used in cable barrier systems. *Proceedings of the 11th International LS-DYNA Users Conference*, Detroit, 6–0 July 2010.
- WALEWSKI, J. 1965. Zasady projektowania kopalń. Część V, Projektowanie szybów i szybków (The principles for the design of mines. Part V, Design shafts and foreshafts) Wydawnictwo Śląsk, Katowice. ◆